J. Fluid Mech. (1979), *vol.* 94, *part* 1, *pp.* 83–101
Printed in Great Britain

Measurements of concentration fluctuations in relative turbulent diffusion

By P. C. CHATWIN AND PAUL J. SULLIVAN†

Department of Applied Mathematics and Theoretical Physics, University of Liverpool

(Received 20 April 1978 and in revised form 19 February 1979)

In 1965 Sullivan made many measurements of concentration in dye plumes in the surface layer of Lake Huron with the primary purpose of estimating the distance–neighbour function (Sullivan 1965, 1971). This paper presents the results of a recent analysis of the concentration fluctuations in these experiments for, despite their great practical and theoretical importance, there are very few published reports of such measurements from natural environments. One reason for this apparent neglect has undoubtedly been the anticipated high noise level, and the present results confirm this expectation. The experimental analysis uses the framework of relative diffusion since this has great advantages compared with that of absolute diffusion. Despite the noise, the results are consistent, to the degree of spatial resolution attained, with the self-similar structure anticipated for relative, but not absolute, diffusion. Further interesting features of the results are that changes in the form of the statistical properties across the plume indicate an unexpectedly strong influence of the central regions, and that certain statistical properties have much less noisy profiles than that of the mean square fluctuations. The influence of molecular diffusion is shown to be strong. Interpretation of the results is based partly on the extension of the theory recently developed by Chatwin & Sullivan (1979*a*) for a cloud, although the limited spatial resolution attained did not allow direct critical examination of this work.

1. Introduction

In most practical cases of turbulent diffusion, like the spillage of a toxic chemical or the release of an obnoxious gas, knowledge of the distribution of the ensemble mean concentration $C(\mathbf{x},t)$ is not adequate to answer most of the important questions. At the very least, knowledge of the distribution of $\overline{c^2}(\mathbf{x},t)$, where $c(\mathbf{x},t)$ is the concentration fluctuation [that is the difference between $\Gamma(\mathbf{x},t)$, the actual concentration in one realization, and $C(\mathbf{x},t)$], is desirable, since it is the variance at position $\mathbf{x}$ and time t of the probability density function of Γ. This remark is reinforced by observations which suggest that $(\overline{c^2})^{\frac{1}{2}}$ is invariably at least of the same order as C (Murthy & Csanady 1971).

However, relatively few observations of $\overline{c^2}$, or any other statistical properties of c, have been reported. Most of these have been taken in the laboratory and analysed within the framework of absolute diffusion, that is with $\mathbf{x}$ measured relative to a fixed origin (e.g. Uberoi & Corrsin 1953; Crum & Hanratty 1965). Interesting and important

† Permanent address: Department of Applied Mathematics, University of Western Ontario, London, Canada.

0022-1120/79/4301-7410 $02.00

though such experiments are, it is, for several reasons, difficult to infer from them valid or useful predictions for the large-scale dispersion phenomena normally encountered in the atmosphere, the oceans and similar environments. Primarily this is because the most substantial contribution to the dispersion of a cloud or plume in absolute diffusion comes from the energy-containing components of the turbulent velocity field, and the structure of these is strongly dependent upon the large-scale geometry of the flow field. Such dependence will inevitably affect the statistical properties associated with the cloud or plume, such as its mean rate of growth or the magnitudes of quantities like $C(\mathbf{x}, t)$ and $\overline{c^2}(\mathbf{x}, t)$ [although not, apparently, the almost universally observed Gaussian form of $C(\mathbf{x}, t)$!]. A related practical point is that it is frequently impossible in natural environments to measure reliably any statistical properties which depend strongly on these large-scale components. This is brought out very clearly in a discussion of experiments carried out in 1962 in Lake Huron by Csanady (1963), and also by many other authors.

Normally in natural environments the length scale of the energy-containing components of the velocity field is much greater than the instantaneous width of the cloud or plume, so that these components affect only the displacement as a body of the cloud or plume as a whole and not its spreading about its instantaneous centre. Therefore, provided $\mathbf{x}$ is measured relative to the instantaneous centre of mass of a cloud, or the instantaneous centre-line of a plume, the statistical properties of $\Gamma(\mathbf{x}, t)$ are then unaffected by the energy-containing components. The experiments reported in this paper were analysed with $\mathbf{x}$ measured in this way, that is in the framework of relative diffusion (Batchelor 1952*a*; Csanady 1973; Monin & Yaglom 1975). Apart from the elimination of effects of the energy-containing components, relative diffusion has two other important advantages compared with absolute diffusion. First of all it avoids unnecessary smearing of the statistical properties of $\Gamma(\mathbf{x}, t)$. Also if the mean width of the cloud or plume lies well within the inertial subrange of Kolmogoroff (Monin & Yaglom 1975, §21), many statistical properties of $\Gamma(\mathbf{x}, t)$ will, when suitably scaled, be universal (i.e. independent of the Reynolds number and the flow geometry). These are described in detail in §24 of Monin & Yaglom (1975). Large inertial subranges exist however only in the very high Reynolds number flows encountered in natural environments.

Experiments on dye plumes in Lake Huron were made by Sullivan in 1965 with the purpose of measuring $C(\mathbf{x}, t)$ and the distance–neighbour function (Sullivan 1965, 1971, 1975). The Reynolds number was high enough in each case for a substantial inertial subrange to exist. In view of this, and also because the measurements were made at more downstream locations than in the very few other similar experiments reported [nine compared with, for example, the four of Murthy & Csanady (1971)], the profiles of the concentration fluctuations have recently been extracted from the experimental records and are presented here. Although the profiles are inevitably noisy they do suggest strongly that, to the degree of spatial resolution attained, $\overline{c^2}$ develops in a self-similar way. It is also shown that these noisy profiles yield much more stable profiles of some other statistical properties, whose consideration and interpretation is a novel feature of this paper.

The experimental results are discussed in terms of a new description of the statistical structure of a steady plume, analogous to that presented for a cloud by Chatwin &

Sullivan (1979*a*). However, because of the limited spatial resolution attained in the experiments, much of this description could not be directly examined.

2. Experimental results

In each experiment a dye plume was formed in the well-mixed surface layer of Lake Huron by the injection of a neutrally buoyant solution of Rhodamine B dye at a constant rate. A small boat carrying fluorometric equipment was used to traverse the plume repeatedly in a direction normal to the instantaneous plume axis. During each experiment the flow conditions were almost steady, and the angle between the instantaneous plume axis and the mean current was small, certainly never greater than 10°. Vertical diffusion of the dye was limited by the presence of the thermocline so that only the spreading of the dye in the horizontal was considered to be important, and the measurements were analysed on this basis. Up to 25 crossings were made at each of nine locations (one or two for each of the five plumes). For each location measurements of concentration were made 1 m below the surface; also at three of these locations measurements were made simultaneously at 2 m below the surface. Thus measurements were made at a total of 12 stations.

The current speed and thermocline depth varied from experiment to experiment, but in all cases the Reynolds number based on these parameters was greater than 10^6. The value of ϵ, the mean rate of dissipation of energy per unit mass, was estimated very approximately by Sullivan (1971) to have an average over the experiments of $2{\cdot}1 \times 10^{-7}\,\mathrm{m^2\,s^{-3}}$, using methods summarized on p. 566 of Monin & Yaglom (1975). Using values of $10^{-6}\,\mathrm{m^2\,s^{-1}}$ for ν (the kinematic viscosity) and $10^{-9}\,\mathrm{m^2\,s^{-1}}$ for κ (the molecular diffusivity), the viscous cut-off length $(\nu^3/\epsilon)^{\frac{1}{4}}$ and the conduction cut-off length $(\kappa^2\nu/\epsilon)^{\frac{1}{4}}$ were then estimated to be $1{\cdot}5 \times 10^{-3}$ m and $4{\cdot}7 \times 10^{-5}$ m respectively. At the sampling stations, the plume widths varied from 16 m to 80 m, while the diameter of the tube injecting the dye was $6{\cdot}35 \times 10^{-2}$ m. The overall resolution of the fluorometric equipment and the digitization procedure used in analysing the data was estimated to be to a length scale of about 4 m.

Further details of the flow conditions and experimental equipment are given in Sullivan (1965, 1971).

Denote by x and y horizontal distances measured respectively along the instantaneous plume axis from the source, and normal to the axis. At each station a number n of crossings were made and, for each crossing, a digitized record of the distribution of concentration Γ_i $(1 \leqslant i \leqslant n)$ was obtained as a function of y. Note that n varied from station to station. Each such record was normalized to have unit integral and, since relative diffusion was being studied, the origin of y was, for each crossing, chosen to be the centre of mass. Thus, for $1 \leqslant i \leqslant n$,

$$\int_{-\infty}^{\infty} \Gamma_i(x,y)\,dy = 1 \quad \text{and} \quad \int_{-\infty}^{\infty} y\Gamma_i(x,y)\,dy = 0. \tag{2.1}$$

At each of the 12 stations, the ensemble mean concentration $C(x,y)$ and the mean width $L(x)$ were determined by

$$C(x,y) = n^{-1} \sum_{i=1}^{n} \Gamma_i(x,y) \tag{2.2}$$

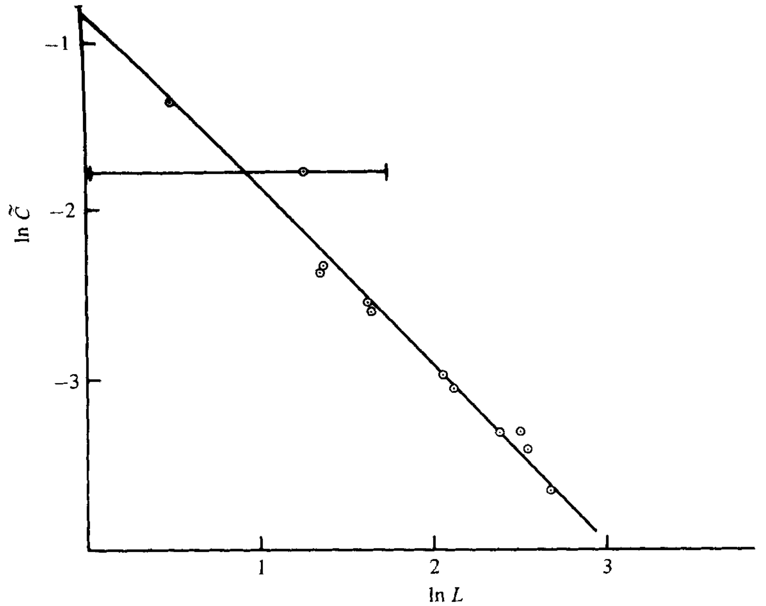

FIGURE 1. The variation of $\tilde{C}$ with L. The straight line is the curve $\tilde{C} = 0{\cdot}436L^{-1{\cdot}03}$ and the error bar shows, for one station, the magnitude of the root-mean-square variation of L about its mean. (One unit of L is equal to 3·36 m.)

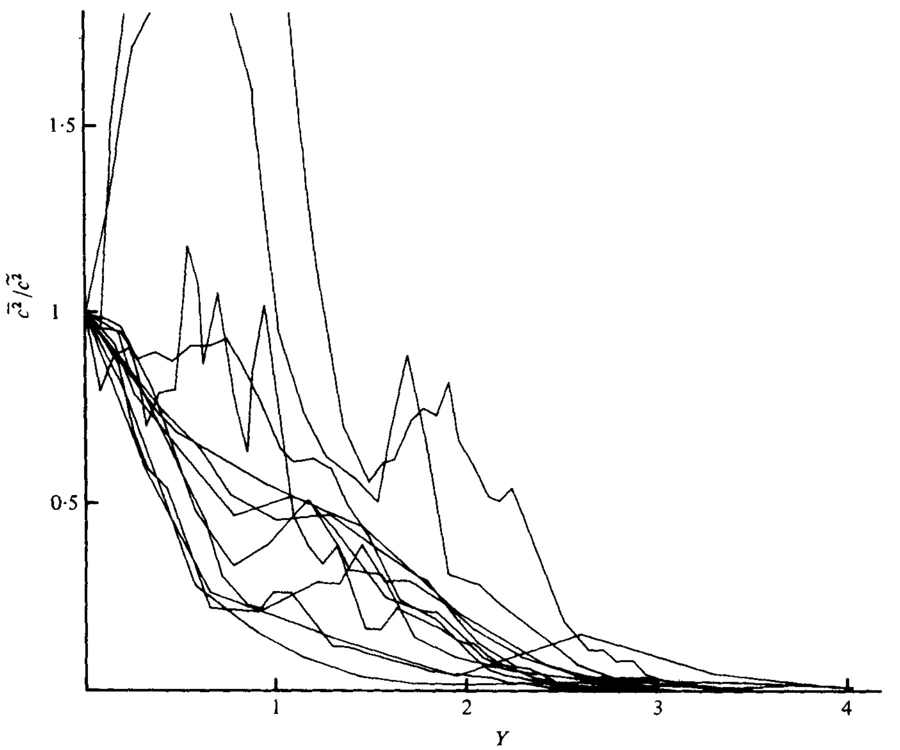

FIGURE 2. The variation of $\overline{c^2}(x, Y)/\tilde{c}^2$ with Y for each of the 12 stations.

Station	Numbers of crossing	f					
		μ_2	μ_4	μ_6	μ_4/μ_2^2	μ_6/μ_2^3	$\mu_6/\mu_4^{\frac{3}{2}}$
1–1	25	0·92	2·24	10·2	2·70	13·3	3·04
1–2*	8	1·10	4·60	37·5	3·80	28·0	3·80
2–1*	25	1·46	8·35	61·0	3·90	20·0	2·52
2–2	20	0·66	1·75	7·5	4·00	26·1	3·23
3–1U*	26	1·22	10·60	126·0	7·40	69·5	4·35
3–1L	27	1·30	5·40	44·8	3·22	20·4	3·58
3–2U	16	0·97	2·80	12·7	3·00	14·2	2·73
3–2L	16	1·14	3·95	21·9	3·05	14·7	2·80
4–1U*	12	1·03	2·96	13·0	2·80	11·8	2·55
4–1L*	9	1·18	4·62	40·5	3·33	24·7	4·10
4–2*	10	1·90	10·00	68·5	2·76	10·0	2·16
5–1	15	1·18	3·92	17·3	2·85	10·5	2·22
All stations							
	$\bar{f} = \frac{1}{12}\Sigma f$	1·17	5·10	38·4	3·57	21·9	3·09
	$\overline{(f-\bar{f})^2}/(\bar{f})^2$	0·06	0·31	0·73	0·12	0·50	0·05
Excluding starred stations							
	$\bar{f} = \frac{1}{6}\Sigma f$	1·03	3·34	19·1	3·14	16·5	2·93
	$\overline{(f-\bar{f})^2}/(\bar{f})^2$	0·04	0·14	0·42	0·02	0·10	0·02
			Gaussian values		3	15	2·89 ($= 5/\sqrt{3}$)

$$\mu_n = \int_{-\infty}^{\infty} Y^n \overline{c^2}(x, Y)\, dY \Big/ \int_{-\infty}^{\infty} \overline{c^2}(x, Y)\, dY.$$

TABLE 1. Some integral moments of $\overline{c^2}$. In the specification of the stations, the first number refers to the plume, the second to the downstream location and the letters U or L to upper or lower reading levels. (See the text.) The data from starred stations was considered less reliable than from the others either because the plume was too thin to permit reasonable accuracy or because the number of crossings was small.

and

$$L^2(x) = \int_{-\infty}^{\infty} y^2 C(x,y)\, dy. \tag{2.3}$$

The form of $C(x,y)$ at each station was approximately a Gaussian function of y (Sullivan 1971). Figure 1 shows how $C(x, 0)$ decreases as $L(x)$ increases. Note that in figure 1 a tilde is used, as it will be throughout this paper, to denote the value of any experimentally determined function $f(x,y)$ on $y = 0$. Thus

$$\tilde{f} = \tilde{f}(x) = f(x, 0). \tag{2.4}$$

[No graph showing the variation of $L(x)$ with x is given because conditions, while steady during each experiment, varied greatly from day to day. In these circumstances no verification of Richardson's law was expected or obtained. Values of x, ranging from 140 m to 500 m, were measured and are given in Sullivan (1971).]

The fluctuation of concentration in each crossing $c_i(x,y)$ was obtained by

$$c_i(x,y) = \Gamma_i(x,y) - C(x,y), \tag{2.5}$$

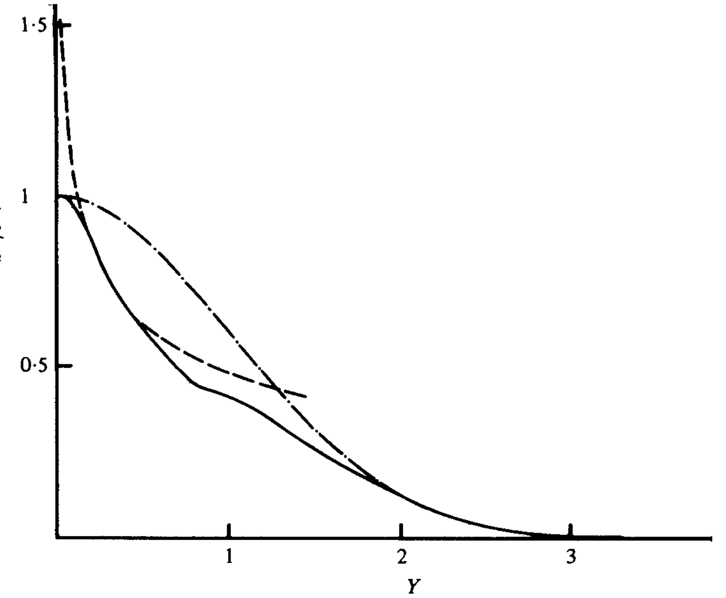

FIGURE 3. The solid line is $\langle \overline{c^2}(x, Y)/\widetilde{c^2}\rangle$, the dashed line is $0{\cdot}49\,Y^{-0{\cdot}35}$ and the dash-dotted line is $\exp(-\frac{1}{2}Y^2)$.

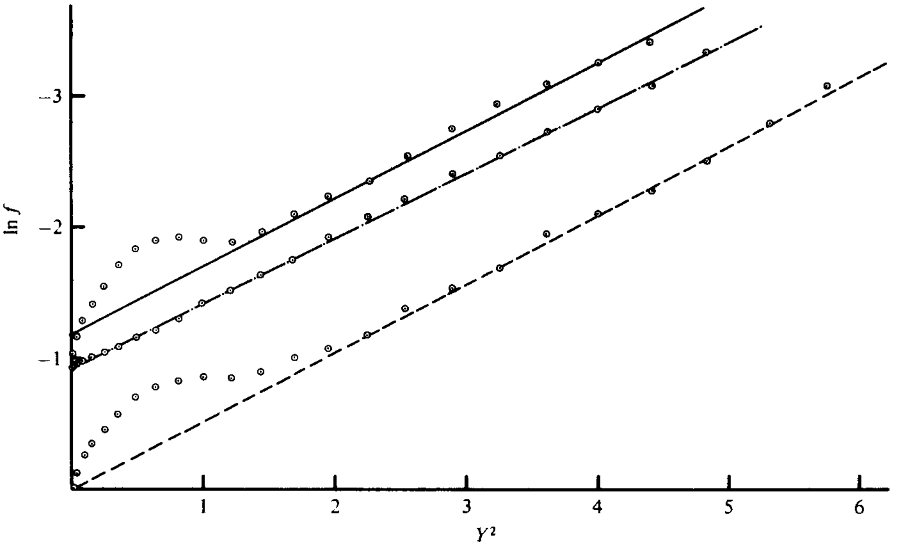

FIGURE 4. A demonstration that $\langle L\overline{c^2}\rangle$ (——), $\langle LC\rangle$ (—·—) and $\langle \overline{c^2}/\widetilde{c^2}\rangle$ (-----) are all proportional to $\exp(-\frac{1}{2}Y^2)$ for large enough Y.

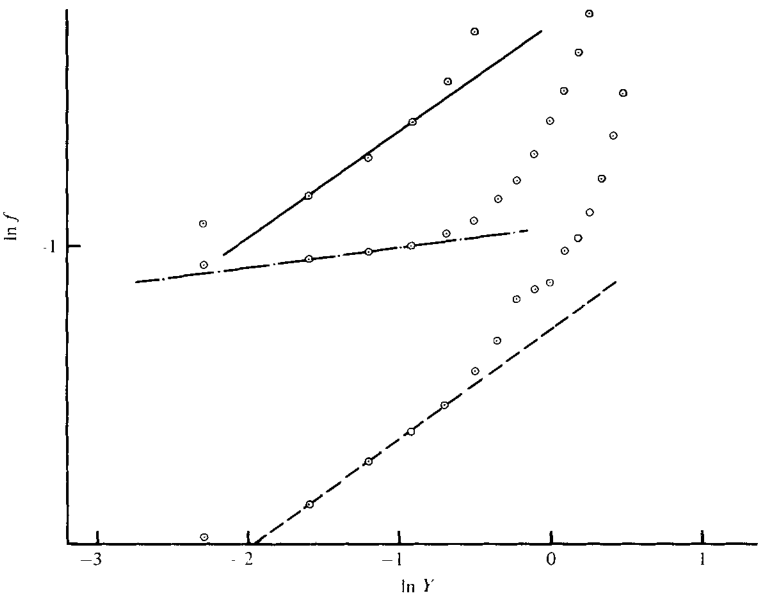

FIGURE 5. A demonstration that $\langle L\overline{c^2}\rangle$ (——), $\langle LC\rangle$ (—·—) and $\langle \overline{c^2}/\widetilde{c^2}\rangle$ (– – – –) all behave like power laws for the smallest values of Y observed.

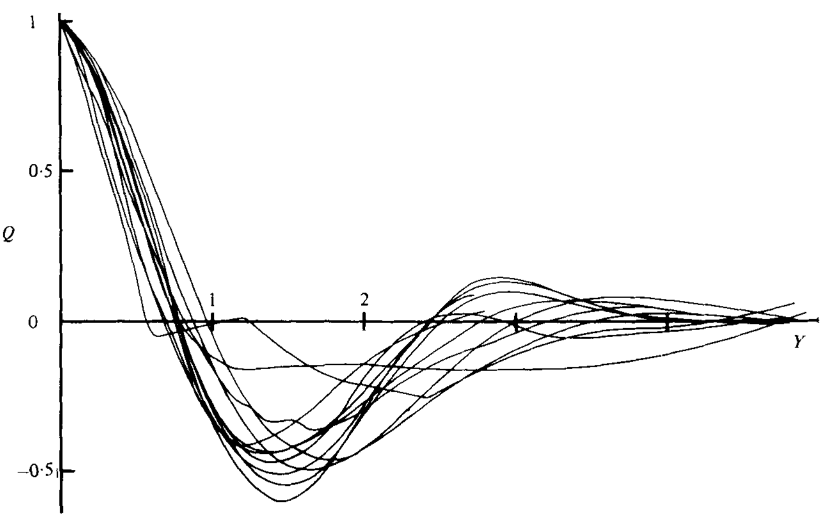

FIGURE 6. The variation of $Q(x, Y)$ with Y for each of the 12 stations.

and $\overline{c^2}(x,y)$ was determined for each station by

$$\overline{c^2}(x,y) = n^{-1}\sum_{i=1}^{n} c_i^2(x,y). \tag{2.6}$$

Figure 2 plots $\overline{c^2}(x, Y)/\widetilde{c^2}(x)$ against Y for each of the 12 stations, where

$$Y = y/L(x). \tag{2.7}$$

Table 1 lists some integral moments of $\overline{c^2}(x, Y)$ together with corresponding values

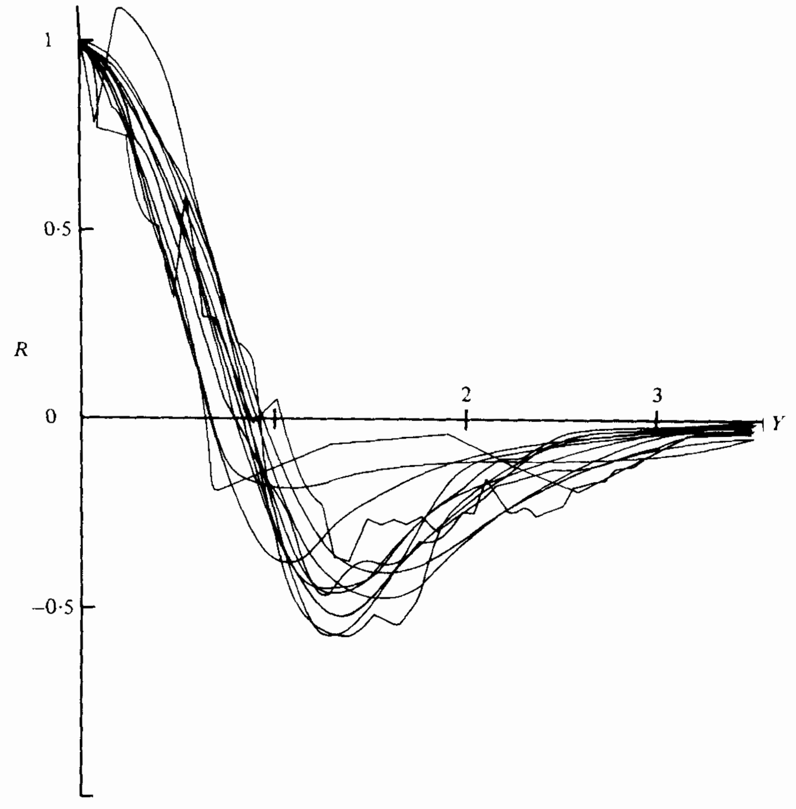

FIGURE 7. The variation of $R(x, Y)$ with Y for each of the 12 stations.

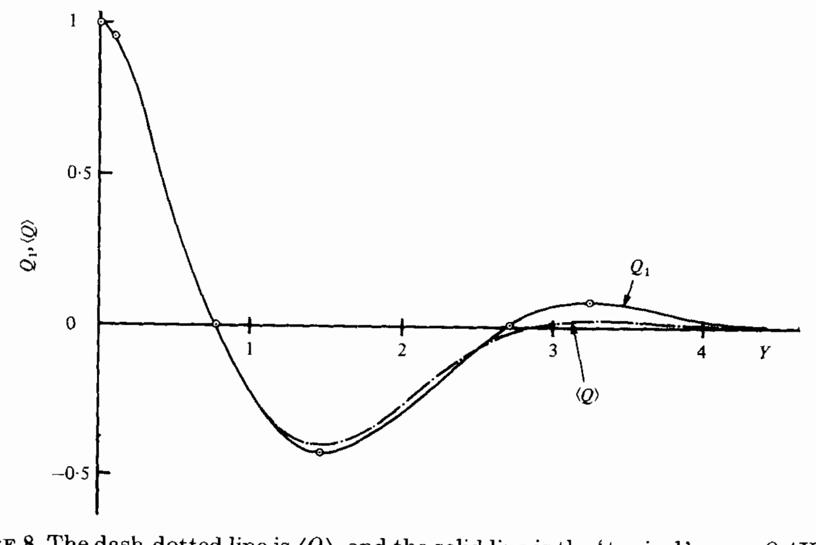

FIGURE 8. The dash-dotted line is $\langle Q \rangle$, and the solid line is the 'typical' curve $Q_1(Y)$ (see table 2).

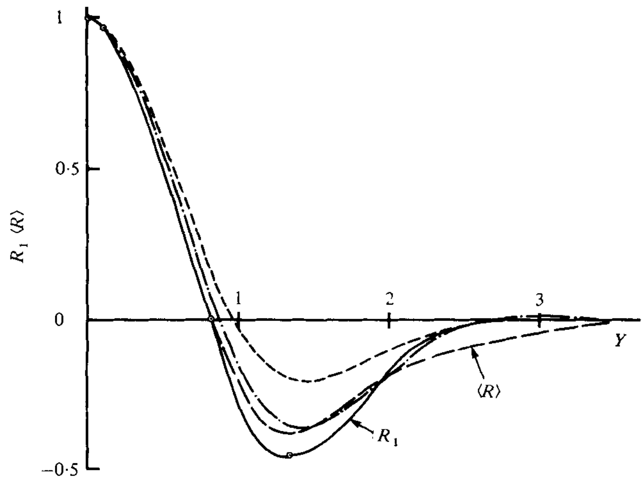

FIGURE 9. The long-dashed line is $\langle R \rangle$, the solid line is the 'typical' curve $R_1(Y)$ (see table 2), the short-dashed line is $\cos(1{\cdot}6Y)\exp(-0{\cdot}579Y^2)$ and the dash-dotted line is $\cos(1{\cdot}8\,Y) \times \exp(-0{\cdot}414Y^2)$.

$$Q_1(Y) = \sum_{n=0}^{8} A_n\, Y^{2n} e^{-Y^2} \quad (\text{with } A_0 = 1)$$

(i) $Q_1(0{\cdot}1) = \langle Q(x, 0{\cdot}1)\rangle$;
(ii) $Q_1(Y_1) = Q_1(Y_2) = 0$, where Y_1 and Y_2 are the average values of the two zeros of Q in figure 6;
(iii) $Q_1'(Y_3) = Q_1'(Y_4) = 0$, where Y_3 and Y_4 are the average values of the positions of the minima and maxima respectively in figure 6;
(iv) $Q_1(Y_3) = \alpha$ and $Q_1(Y_4) = \beta$, where α and β are the averages of the minima and maxima respectively in figure 6;
(v) $\int_0^\infty Q_1(Y)\,dY = 0$ [see equation (3.15)].

$$R_1(Y) = \sum_{n=0}^{5} B_n\, Y^{2n} e^{-2Y^2} \quad (\text{with } B_0 = 1)$$

(i) $R_1(0{\cdot}1) = \langle R(x, 0{\cdot}1)\rangle$;
(ii) $R_1(Y_1) = 0$, where Y_1 is the average value of the zeros of R in figure 7;
(iii) $R_1'(Y_2) = 0$, where Y_2 is the average value of the position of the minima in figure 7;
(iv) $R_1(Y_2) = \alpha$, where α is the average of the minima in figure 7;
(v) $\int_0^\infty R_1(Y)\,dY = 0$ [see (3.15)].

TABLE 2. The forms of the 'typical' curves $Q_1(Y)$ and $R_1(Y)$, and the specific properties satisfied by them.

from a Gaussian curve, and some measures of their variability. Figure 3 shows how $\langle \overline{c^2}(x, Y)/\widetilde{c^2}(x)\rangle$ varies with Y, where the angle brackets denote, as they will throughout this paper, an average over all 12 stations. Figure 3 also contains a comparison of $\langle \overline{c^2}(x, Y)/\widetilde{c^2}(x)\rangle$ with two simple functions, obtained in the ways shown on figures 4 and 5 respectively.

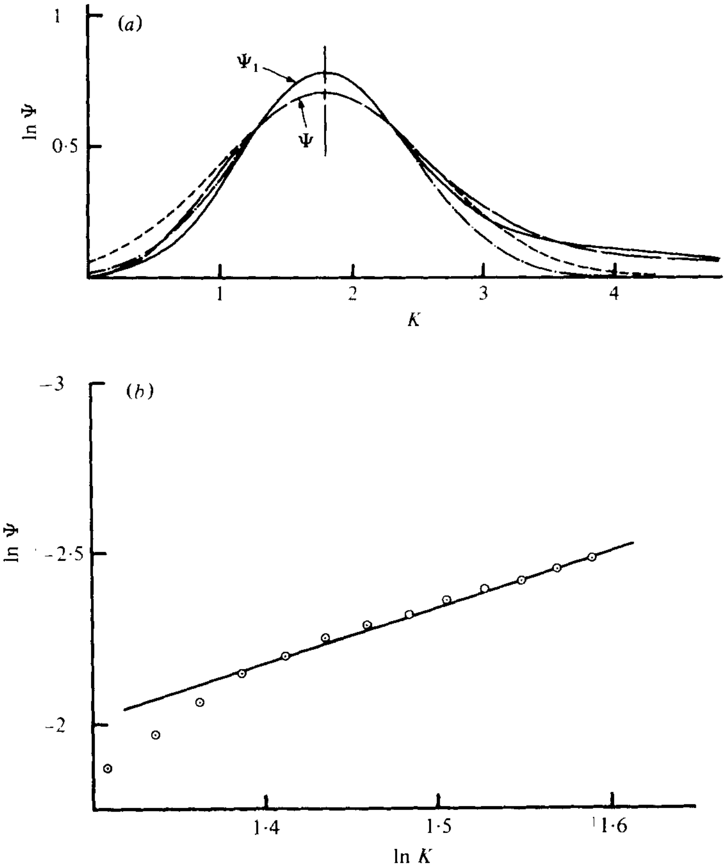

FIGURE 10. (a) The Fourier transforms of $\langle Q \rangle$ and Q_1: the long-dashed line is $\Psi(K)$ and the solid line is $\Psi_1(K)$, both defined in (2.10); the short-dashed line is $0{\cdot}70 \exp\{-0{\cdot}78(K-1{\cdot}8)^2\}$ and the dash-dotted line is $0{\cdot}78 \exp\{-1{\cdot}17(K-1{\cdot}8)^2\}$. (b) shows that $\Psi(K) = 1{\cdot}19K^{-\frac{5}{3}}$ for $K \gtrsim 3{\cdot}5$.

The records of $c_i(x, Y)$ were then used to determine two other statistical functions $Q(x, Y)$ and $R(x, Y)$ defined for each station by

$$Q(x, Y) = \int_{-\infty}^{\infty} \overline{c(x, Y')\,c(x, Y+Y')}\,dY' \Big/ \int_{-\infty}^{\infty} \overline{c^2}(x, Y')\,dY', \tag{2.8}$$

$$R(x, Y) = \overline{c(x, 0)\,c(x, Y)}/\widetilde{c^2}. \tag{2.9}$$

The forms of Q and R for each of the 12 stations are shown in figures 6 and 7 respectively, while $\langle Q \rangle$ and $\langle R \rangle$ are shown in figures 8 and 9. Also shown in the latter figures are 'typical' functions $Q_1(Y)$ and $R_1(Y)$ obtained by fitting curves so that they satisfied properties characteristic of the separate curves in figures 6 and 7. Details are given in table 2. The reason for believing that $Q_1(Y)$ and $R_1(Y)$ may give truer pictures than $\langle Q \rangle$ and $\langle R \rangle$ is that the latter contain the unwanted effect of unknown errors in the measured values of $L(x)$. Not only are there unavoidable (though presumably unbiased) statistical errors indicated by an error bar in figure 1, but also the possibility that the measured values of $L(x)$ are consistently too high because the plume is not traversed exactly at right angles to its instantaneous axis. These errors, particularly important at large values of Y, *could* explain all the scatter in the separate curves in figures 6 and 7, and lead to curves of $\langle Q \rangle$ and $\langle R \rangle$ in figures 8 and 9 that are too smeared. The technique used to obtain Q_1 and R_1 attempts to avoid this smearing while retaining the prominent features of the separate curves. Figure 10(*a*) shows the Fourier transforms of $\langle Q \rangle$ and Q_1 defined, since Q is even from (2.8), by

$$\Psi(K) = \int_0^\infty \langle Q(x, Y) \rangle \cos(KY)\, dY, \quad \Psi_1(K) = \int_0^\infty Q_1(Y) \cos(KY)\, dY. \tag{2.10}$$

Figure 10(*b*) shows that $\Psi(K)$ is proportional to $K^{-\frac{5}{3}}$ for $K \gtrsim 3{\cdot}5$.

3. A theoretical framework

Consider one realization of the dispersion, and choose as origin the point on the instantaneous centre-line at the section where measurements are taken. Let $\boldsymbol{\Upsilon}(\mathbf{x}, t)$ be the fluid velocity relative to the velocity of this (randomly) moving origin. The equation governing $\Gamma(\mathbf{x}, t)$ is then

$$\partial \Gamma / \partial t + \nabla . (\boldsymbol{\Upsilon} \Gamma) = \kappa \nabla^2 \Gamma. \tag{3.1}$$

Express $\boldsymbol{\Upsilon}$ and Γ in terms of their ensemble means (denoted by overbars) and fluctuations as follows:

$$\boldsymbol{\Upsilon} = \mathbf{U}(\mathbf{x}) + \mathbf{u}(x, t), \quad \Gamma = C(\mathbf{x}) + c(\mathbf{x}, t), \quad \text{where} \quad \bar{\mathbf{u}} = \mathbf{0}, \quad \bar{c} = 0. \tag{3.2}$$

The notation in (3.2) explicitly indicates that $\mathbf{U}$ and C are independent of time because the turbulence is stationary and because the contaminant is injected at a constant rate. Substitution of (3.2) into (3.1) leads, in the normal way, to the following equations for C and c:

$$\nabla . (\mathbf{U}C + \overline{\mathbf{u}c}) = \kappa \nabla^2 C; \tag{3.3}$$

$$\frac{\partial c}{\partial t} + \nabla . (\mathbf{U}c + \mathbf{u}C + \mathbf{u}c - \overline{\mathbf{u}c}) = \kappa \nabla^2 c. \tag{3.4}$$

The equation for $\overline{c^2}$, which is also independent of time, is obtained from (3.4) by multiplying by $2c$ and taking the ensemble mean. After rearranging it becomes

$$\mathbf{U} . \nabla \overline{c^2} + \nabla . (\overline{\mathbf{u}c^2}) + 2\overline{\mathbf{u}c} . \nabla C = \kappa \nabla^2 \overline{c^2} - 2\kappa \overline{(\nabla c)^2}. \tag{3.5}$$

Except for using the steadiness of C and $\overline{c^2}$ these equations are quite general. But it is now time to use the special features of the experimental situation to simplify them. With x measured along the instantaneous centre-line, y measured horizontally and normal to this line, and z measured vertically, $\mathbf{U} = (U, 0, 0)$, where U is the mean current, independent of t. Since the vertical diffusion of the dye is limited by the thermocline, as explained in § 2, it will be supposed that no mean values depend on z or, equivalently, that all ensemble means appearing from now on can be regarded as averages of the previous ensemble means over the vertical. Also the length scale of variations of C and $\overline{c^2}$ in the streamwise direction is much greater than that in the direction across the plume so that boundary-layer approximations can be made, typified by neglecting $\partial(\overline{u_x c^2})/\partial x$ in comparison with $\partial(\overline{u_y c^2})/\partial y$. Hence (3.3) and (3.5) can be approximated by

$$U\frac{\partial C}{\partial x}+\frac{\partial}{\partial y}\overline{(u_y c)} = \kappa\frac{\partial^2 C}{\partial y^2} \tag{3.6}$$

and

$$U\frac{\partial \overline{c^2}}{\partial x}+\frac{\partial}{\partial y}\overline{(u_y c^2)}+\overline{2u_y c}.\frac{\partial C}{\partial y} = \kappa\frac{\partial^2 \overline{c^2}}{\partial y^2}-2\kappa\overline{\left(\frac{\partial c}{\partial y}\right)^2}. \tag{3.7}$$

An immediate consequence of (3.6) is that, for all x,

$$\int_{-\infty}^{\infty} C\,dy = M, \tag{3.8}$$

where M is a constant such that MU is the steady rate of emission of contaminant per unit depth. In the analysis of the experiments M was, without loss of generality, taken to be 1 [see equation (2.1)].

The dispersion of a plume of marked fluid particles ($\kappa = 0$)

It is valuable, as a preliminary, to examine some consequences of (3.6) and (3.7) when $\kappa = 0$. Putting $\kappa = 0$ in (3.7) and integrating over all y gives

$$U\frac{d}{dx}\int_{-\infty}^{\infty}\overline{c^2}\,dy = -2\int_{-\infty}^{\infty}\overline{u_y c}\frac{\partial C}{\partial y}\,dy = -2U\int_{-\infty}^{\infty} C\frac{\partial C}{\partial x}\,dy,$$

on using (3.6) with $\kappa = 0$. Thus, for all x,

$$\int_{-\infty}^{\infty} C^2\,dy+\int_{-\infty}^{\infty}\overline{c^2}\,dy = \frac{M^2}{L_0}, \tag{3.9}$$

where M is defined in (3.8) and L_0 is a constant length determined entirely by the initial conditions and of the same order as the diameter of the tube injecting the contaminant.†

Since conditions at the source are the same in each realization $c(0,y) = 0$, and thus $\overline{c^2}(0,y) = 0$. Hence for sufficiently small x, the integral of $\overline{c^2}$ in (3.9) is small compared with the integral of C^2. But this state of affairs reverses as x increases, for eventually the magnitude of C is of order M/L (as shown in figure 1 for the experiments analysed in this paper). Thus eventually

$$\int_{-\infty}^{\infty} C^2\,dy \propto M^2/L, \tag{3.10}$$

and this becomes negligible. Hence eventually the integral of $\overline{c^2}$ dominates the left-hand side of equation (3.9). When this happens the only possibility is that the magnitude of $\overline{c^2}$ is of order M^2/LL_0 in most of the plume; if also the distribution of $\overline{c^2}$, like that of C, is self-similar in most of the plume, then

$$\overline{c^2} \approx \frac{M^2}{LL_0}J(Y), \tag{3.11}$$

where Y is defined in (2.7). This result, a new one, shows that, when the effects of κ are negligible, the initial conditions influence the statistical properties of c for all x. It

† In these experiments L/L_0 was of order 10^2, according to the data at the beginning of §2.

follows that theoretical analyses of concentration fluctuations can have no validity unless such influence is included. In particular, it would be meaningless to model the source as a point, and there is no justification (even if effects of κ are modelled) for assuming $\overline{c^2} = (M^2/L^2)J(Y)$, as was done by Csanady (1973, p. 236).

A consequence of this result is very surprising however. From (3.6) with $\kappa = 0$, it follows that $\overline{u_y c}$ has the same sign as Y (since $\partial C/\partial x$ is negative), that is the transfer of C is everywhere outwards from the centre-line. It also follows that $\overline{u_y c}$ has order of magnitude (UML'/L), where $L' = dL/dx$, so that the production term in (3.7), namely $2\overline{u_y c}(\partial C/\partial y)$, has order of magnitude (UM^2L'/L^3). But, according to (3.11), the advection term in (3.7), namely $(U\partial\overline{c^2}/\partial x)$, has order of magnitude (UM^2L'/L^2L_0). The distribution of $\overline{c^2}$ is therefore determined by a balance between advection and transfer whenever (3.11) holds, with the production of $\overline{c^2}$ everywhere negligible. As well as being novel, this conclusion is difficult to accept since it requires the integral of $\overline{c^2}$ over all y to be independent of x. But it is easy to show from (3.7) that it also requires that the transfer of $\overline{c^2}$, namely $\overline{u_y c^2}$, is everywhere outwards from the centre-line, just like the transfer of C. This suggests one possible resolution of the difficulty,† which is that the $\overline{c^2}$ which is transferred outwards is produced in a small central region, to be called the core. Within the core, the production of $\overline{c^2}$ must be comparable to its advection and transfer, and this requires the magnitude of $\overline{c^2}$ in the core to be much greater than in (3.11). The thickness of the core has to tend to zero as x tends to infinity so that the integral of $\overline{c^2}$ over the core is small compared with the integral over the bulk of the plume where (3.11) holds.

For the case of a diffusing finite cloud a result analogous to (3.11) holds, and leads to a similar difficulty about the production of $\overline{c^2}$. It was shown by Chatwin & Sullivan (1979*a*) that a core–bulk structure, analogous to that described above, is the correct resolution of this difficulty when the velocity field is a pure straining motion. Other arguments, essentially geometrical, show that this structure also exists with some other velocity fields. But whether such a structure exists in all cases is an unsolved, but important, problem.

The effects of molecular diffusion

One effect of turbulence is to tend to distort volume elements into thin sheets or long cylinders. Consider a volume element containing marked fluid. The distortion causes the maximum gradient of concentration within the element, and its surface area, to increase with time on the average. Hence the smoothing effect of κ on the statistical properties of Γ also increases with time (which is equivalent to distance downstream from the source for a steady plume). Batchelor (1952*b*, 1959) argued that eventually there is a balance between the competing effects of advection and molecular diffusion which prevents the minimum dimensions of the sheets or cylinders into which volume elements are distorted becoming less than a length of order $(\kappa^2\nu/\epsilon)^{\frac{1}{4}}$, the conduction cut-off length. Batchelor's conclusion was confirmed for the case of an initial sphere of marked fluid being distorted by a pure straining motion by Chatwin & Sullivan (1979*a*).

† Another possible resolution, suggested by a referee, may hold in certain circumstances. This is that essentially all production of $\overline{c^2}$ takes place so near the source that, contrary to the assumptions made above, C and $\overline{c^2}$ are *not* of order M/L and M^2/LL_0.

In the experiments analysed in this paper $L_0 > 1000(\kappa^2\nu/\epsilon)^{\frac{1}{4}}$, so the effect of κ will not become significant until some distance downstream from the source (Chatwin & Sullivan 1979*a*). But for large enough x, the effect is profound. In particular it is easy to show from (3.7) that, when $\kappa \neq 0$,

$$\lim_{x\to\infty}\left\{\int_{-\infty}^{\infty} C^2\,dy+\int_{-\infty}^{\infty}\overline{c^2}\,dy\right\} = 0,$$

in contrast with (3.9). Thus

$$\lim_{x\to\infty}\left\{\int_{-\infty}^{\infty}\overline{c^2}\,dy\right\} = 0, \tag{3.12}$$

and not M^2/L_0, its value when $\kappa = 0$. Eventually, therefore, the magnitude of $\overline{c^2}$ must be less by an order of magnitude than M^2/LL_0, the value given in (3.11) for $\kappa = 0$. It is *not yet known how κ affects $\overline{c^2}$ more precisely. But speculative arguments, already* used in the analogous situation for a finite cloud by Chatwin & Sullivan (1979*a*), suggest that there are non-dimensional numbers A and n so that, sufficiently far downstream,

$$\frac{d}{dx}\int_{-\infty}^{\infty}\overline{c^2}\,dy = -A\kappa M^2U^{-1}L^{-n}\left(\frac{\kappa^2\nu}{\epsilon}\right)^{\frac{1}{4}(n-3)}. \tag{3.13}$$

The arguments, based partly on the behaviour of a cloud in pure straining motion, suggest that n is between 1 and 2, and is likely to be nearer 2.

In the absence of κ, the value of $\overline{c^2}$ in the bulk of the plume is determined by a balance between advection and transfer outwards. Earlier it was suggested that this transfer is fed by production in a small core region surrounding $Y = 0$ in which the magnitude of $\overline{c^2}$ is much greater than in the bulk. If this description is correct it follows (Chatwin & Sullivan 1979*a*) that the *direct* effect of κ on $\overline{c^2}$ is essentially confined to the core, and that this effect is transferred outwards to the bulk, thereby *indirectly* decreasing the magnitude of $\overline{c^2}$ there in the way described (tentatively) in (3.13). But it is difficult to see why the shape of the $\overline{c^2}$ against Y curve, that is the function J in (3.11), should be noticeably affected by κ.

Although this paper is concerned with fluctuations, it is necessary to note that mass conservation requires that C is of order M/L in the bulk of the plume, irrespective of whether κ has an important effect. This is confirmed by figure 1 (since $\tilde{C}$ is a bulk value, as explained before equation (2.4)).

The functions Q and R

When equation (3.1) is integrated over all y and averaged over the vertical, there results

$$\left(\frac{\partial}{\partial t}+U\frac{\partial}{\partial x}\right)\int_{-\infty}^{\infty}\Gamma\,dy+\frac{\partial}{\partial x}\int_{-\infty}^{\infty}u_x\Gamma\,dy = \kappa\frac{\partial^2}{\partial x^2}\int_{-\infty}^{\infty}\Gamma\,dy,$$

where it is not necessary to show explicitly the averaging over z since, as explained earlier, only spreading in the horizontal direction is considered to be important. To a first approximation the dominant term in this equation is the first, so that

$$\int_{-\infty}^{\infty}\Gamma\,dy \approx f(x-Ut).$$

This is a mathematical statement of the hypothesis commonly made in analysing dispersing plumes, namely that changes with time at a fixed point occur predominantly as the result of advection with the mean stream. Here with a steady source, f is equal to the constant M defined in (3.8). But, using (3.8) and the decomposition of Γ into mean and fluctuation, it now follows that for each instant

$$\int_{-\infty}^{\infty} c(x,y)\,dy \approx 0. \tag{3.14}$$

[For a finite cloud the integral of c over all space is exactly zero as shown in Chatwin & Sullivan (1979*a*).] From (3.14) it follows immediately that

$$\int_{-\infty}^{\infty} Q(x,Y)\,dY \approx 0, \quad \int_{-\infty}^{\infty} R(x,Y)\,dY \approx 0, \tag{3.15}$$

where Q and R are defined in (2.8) and (2.9) respectively.

Further discussion of the properties of Q is contained in Chatwin & Sullivan (1979*b*). In particular it is shown there that Q has the remarkable property

$$\int_{-\infty}^{\infty} Y^2 Q(x,Y)\,dY \approx 0, \tag{3.16}$$

independently of whether κ is important or, indeed, whether the contaminant is active or passive. This result, unlike (3.15), does not hold in absolute diffusion.

4. The interpretation of the experimental results

Experiments designed to measure the statistical properties of concentration fluctuations require, ideally, more realizations than those designed to measure the ensemble mean concentration. Because experimental errors are inevitably larger, this is even more true in natural environments than in laboratories. Furthermore, relative diffusion experiments in a plume are more difficult than absolute diffusion experiments because of uncertainty about whether the plume is being traversed exactly normal to its instantaneous axis. Perhaps such considerations explain the very few published analyses of both measured statistical properties of concentration fluctuations and relative diffusion experiments. For the reasons given in §1, such neglect is highly unsatisfactory. It is hoped, therefore, that the results presented in this paper, relatively crude though they are, will stimulate more detailed experiments on these topics, so often unjustifiably ignored.

The results have been presented in a way which avoids as far as possible the use of the measured values of L (although these have to be used to determine Y). Values of L are uncertain principally because the correct direction for each plume crossing had to be estimated by eye. Thus all measured values of $\overline{c^2}$, Q and R are normalized by division by their *measured* values at $Y = 0$ so that, unfortunately, the resulting graphs give no information about the magnitudes of these quantities. It is important to stress once more that the measured values are in effect averages over a length scale of about 4 m, so the experimental results do not directly exemplify structure on a scale smaller than this. Obviously therefore they cannot provide direct evidence about a possible core near $Y = 0$, described in §3. Since one property of the core is that the magnitude of $\overline{c^2}$ (and of C) within it is much greater than in the bulk of the plume, a tilde is used in the way explained in connexion with (2.4) to denote measured values at $Y = 0$, so that these will not be confused with real values.

The distribution of $\overline{c^2}$

Figure 2 shows that there is a large amount of noise in the curves of $\overline{c^2}/\widetilde{c^2}$, due principally to the small number of realizations. Nevertheless, the values of the normalized integral moments given in table 1 do appear to be approximately independent of the sampling station, particularly for that subset of the stations that was considered to give the most reliable data. Accordingly it was supposed that the data were consistent with $\overline{c^2}$ having a self-similar form; this confirms the conjecture made by Murthy & Csanady (1971) on the basis of experiments at only four stations. Figure 3 shows the curve of $\langle \overline{c^2}/\widetilde{c^2} \rangle$ obtained by combining the data from all twelve stations, and assuming self-similarity.

From this curve it is evident that $\langle \overline{c^2}/\widetilde{c^2} \rangle$ is Gaussian for $Y \gtrsim 1{\cdot}5$. This is consistent with the closeness of the normalized integral moments given in table 1 with those that would be given by a Gaussian form. For smaller values of Y, which contribute relatively little to the moments, the form of $\langle \overline{c^2}/\widetilde{c^2} \rangle$ is no longer Gaussian. This is particularly evident in figure 4, in which there is also a slight indication that the form of C is no longer Gaussian for small Y. In figure 5, the data are replotted in a way which emphasizes the changes in behaviour of C and $\overline{c^2}$ for small Y, and suggests that the Gaussian forms become power laws. Because of the noisiness of the results, very little significance can be attached to the precise values given in figure 5 for the indices in these power laws. But the change in behaviour of $\overline{c^2}$ for $Y \lesssim 1{\cdot}5$ is very noticeable. Such a change is not predicted by the empirical theory of Csanady (1973, pp. 233–242). That theory makes the assumption that the turbulent transfers of both C and $\overline{c^2}$ can be described using eddy diffusivities, the same for each process. As pointed out following (3.11), the work also unjustifiably supposes that the magnitude of $\overline{c^2}$ is of order M^2/L^2, and one unfortunate prediction based on these assumptions is that $\overline{c^2}$ is negative for $Y \gtrsim 2{\cdot}5$. On the other hand, a marked change in behaviour would be expected if the core–bulk structure proposed in § 3 existed, for then there would be a transition region between the core and the bulk within which the $\overline{c^2}$-stuff produced in the core was being transferred outwards by eddies with length scales of order L. Whether this is the correct explanation cannot be decided, of course, without much more detailed experiments achieving very good spatial resolution.

The functions Q and R

Since $c(x, Y)$ is not a stationary random function of Y, means like

$$\overline{c(x, Y_1)\, c(x, Y_2)} \qquad (4.1)$$

depend on Y_1 and Y_2 separately. Generally it is not therefore possible to use the many techniques developed for stationary random functions and described in § 11 of Monin & Yaglom (1975). But in the present non-stationary process, expressions involving means of products of fluctuations still appear in the hierarchy of equations for the moments of Γ, and the simplest of these have clear physical significance. The functions Q and R defined in (2.8) and (2.9) are especially simple since they depend only on two variables, unlike (4.1) which depends on three variables. Furthermore, Q has direct relation to the distance–neighbour function (Sullivan 1975), and, exceptionally for non-stationary processes, does behave like a correlation function since its Fourier transform must be non-negative everywhere.

For these reasons the data were used to evaluate Q and R for each sampling station with the results shown in figures 6 and 7 respectively. It is remarkable that these curves are much less noisy than the curves of $\overline{c^2}$ in figure 2. Furthermore the same prominent features are observed in the curves of Q and R at each station. Each curve of Q and R has a sensibly zero integral as predicted in (3.15). There seems no reason to doubt that both Q and R have essentially self-similar forms in the bulk of the plume. The straightforward averages $\langle Q\rangle$ and $\langle R\rangle$ are shown in figures 8 and 9 respectively, together with the 'typical' curves Q_1 and R_1, which, for the reasons given in §2, may represent the true curves more closely than $\langle Q\rangle$ and $\langle R\rangle$.

In forming R the centre of the plume is singled out, whereas Q is a measure of structure throughout the plume with all parts being given the same weight. It is therefore very surprising that for $Y \lesssim 2{\cdot}5$ the curves of $\langle Q\rangle$ and $\langle R\rangle$ are almost the same, and it seems that this can occur only if the predominant contribution for $Y \lesssim 2{\cdot}5$ to the integrand in Q comes from pairs of points of which one is near the centre-line, i.e. from those points which determine R. The similarity between $\langle Q\rangle$ and $\langle R\rangle$ for $Y \lesssim 2{\cdot}5$ seems therefore to require the magnitudes of the fluctuations near the centre of the cloud to be substantially higher than elsewhere. Whether they must be as large as required by a core–bulk structure cannot be decided by the present experiments because of the limited spatial resolution. But it seems unlikely that such close similarity would be obtained with magnitudes that decreased at a rate uniform over the whole plume, as conventionally assumed. Whatever the explanation, the negative values of Q and R occur because of transport of material from near the centre out to regions near the periphery by eddies of length scales of order L. Such transport results in changes in c near the centre being of opposite sign to those near the periphery. It is interesting to recall that transport by such eddies was the mechanism suggested earlier for the marked change in behaviour of $\langle \overline{c^2}/\widetilde{c^2}\rangle$ near $Y = 1{\cdot}5$, and to note that this is also the value of Y near which the negative values of Q and R have a maximum. Furthermore, this mechanism causes changes in c near $Y = 1{\cdot}5$ and near $Y = -1{\cdot}5$ to have the same sign; this would explain the shallow maximum of Q near $Y = 3$.

The Fourier transforms of $\langle Q\rangle$ and Q_1, defined as $\Psi(K)$ and $\Psi_1(K)$ in (2.10), are shown in figure 10. For the reasons given earlier, $\Psi(K)$ is a spectrum in the strict sense used in describing stationary random processes. The curves, of course, reflect the general features noted above; in particular $\Psi(0) = \Psi_1(0) = 0$ (corresponding to $\langle Q\rangle$ having zero integral) and both Ψ and Ψ_1 are well fitted by Gaussian curves near their central peaks (corresponding to the Gaussian behaviour noted in the discussion of the graphs of $\overline{c^2}$). However, the main reason for including the figure is to show the $K^{-\frac{5}{3}}$ behaviour of Ψ for $K \gtrsim 3{\cdot}5$. Such behaviour was predicted by Obukhoff (1949) and Corrsin (1951), but only for statistically homogeneous fields of concentration. Perhaps, therefore, the observed behaviour indicates small scale homogeneity of the plume despite the fact that its structure is, by mass conservation, fundamentally inhomogeneous. Noting that $\Psi_1(K)$ does not have the $K^{-\frac{5}{3}}$ behaviour,† Professor A. M.

† Although this is not surprising since $Q_1(Y)$ was fitted to $Q(Y)$ on the basis of large scale features (see table 2), without regard to the small scale features responsible for the $K^{-\frac{5}{3}}$ behaviour of $\Psi(K)$.

Yaglom has suggested to us that an alternative explanation of the behaviour of $\Psi(K)$ for $K \gtrsim 3{\cdot}5$ could be the inaccuracy of the data. Clearly there is need for further investigation.

The effects of molecular diffusion

Arguments at the end of § 3 suggest that the observed self-similarity in the bulk of the plume exists whether or not the effects of κ are important. But the same arguments predict that if κ is important it will strongly affect the magnitudes of all statistical properties except C (which is of order ML^{-1} by mass conservation). Here an attempt is made to examine this point, although no firm conclusions can be reached because of the extensive noise on the data.

Least squares lines of best fit to the data showed that the rates of decrease of $\widetilde{c^2}(x)$ and $\int_0^\infty \overline{c^2}(x,y)\,dy$ with $L(x)$ could be approximated by

$$\widetilde{c^2}(x) \propto L^{-2{\cdot}6}, \quad \int_0^\infty \overline{c^2}(x,y)\,dy \propto L^{-1{\cdot}5}. \tag{4.2}$$

If κ were unimportant these indices would be -1 and 0 respectively, according to (3.11), so that it can be asserted definitely that κ is important in these experiments. Furthermore the observed self-similarity requires that in the bulk of the plume

$$\overline{c^2}(x,y) \approx \widetilde{c^2}(x)\,J(Y) = \widetilde{c^2}(x)\,J(y/L(x)),$$

from which (ignoring the contribution from any core)

$$\int_0^\infty \overline{c^2}(x,y)\,dy \approx \widetilde{c^2}(x)\,L \int_0^\infty J(Y)\,dY. \tag{4.3}$$

Although little reliance can be placed on the exact values of the indices in (4.2), the fact that they differ by approximately 1 is consistent with (4.3). [An indication of the possible sizes of the errors in (4.2) was obtained by calculating the line of best fit to $\widetilde{c^2}(x)/\{\tilde{C}(x)\}^2$, which gave this quantity proportional to $L^{-0{\cdot}8}$, whereas it is proportional to $L^{-2{\cdot}6}/L^{-2} \approx L^{-0{\cdot}6}$ according to (4.2) and figure 1.]

From (4.2) it follows that

$$\frac{d}{dx}\int_{-\infty}^\infty \overline{c^2}(x,y)\,dy \propto L'L^{-2{\cdot}5}. \tag{4.4}$$

Although no direct measurements of x were made for the reason given earlier, $L' \propto L^{\frac{1}{3}}$ since the spreading of the plume is determined by eddies of the relative velocity field lying in the inertial subrange. Thus (4.4) becomes

$$\frac{d}{dx}\int_{-\infty}^\infty \overline{c^2}(x,y)\,dy \propto L^{-2{\cdot}2}, \tag{4.5}$$

approximately. According to (3.13) the left-hand side of (4.5) is proportional to L^{-n}, where n lies between 1 and 2, and is probably closer to 2. In view of the tentative nature both of the theory and the experimental result (4.5), little significance can be attached to the apparent discrepancy.

A note on absolute and relative diffusion

Absolute diffusion experiments in natural environments are, perhaps, more difficult to do than relative diffusion experiments because it is virtually impossible to measure properly those ensemble means that depend on the slow, large scale, energy-containing eddies (and, it was argued in §1, such experiments would also be less useful). In natural environments (unlike some laboratory flows) these eddies are not self-similar and would not, in general, permit the self-similar structure consistent with the present relative diffusion experiments. A more specific difference is that it can be shown from figure 8 that the integral of $Y^2\langle Q\rangle$ over all Y is sensibly zero, consistent with the theoretical result (3.16). This integral is not zero in absolute diffusion (Chatwin & Sullivan 1979*b*).

We are grateful to Professor G. K. Batchelor and to Professor A. M. Yaglom for their very valuable comments on the first draft of this paper. Paul J. Sullivan acknowledges the financial support of the National Research Council of Canada during the period when this work was carried out.

REFERENCES

BATCHELOR, G. K. 1952*a* Diffusion in a field of homogeneous turbulence. II. The relative motion of particles. *Proc. Camb. Phil. Soc.* **48**, 345.

BATCHELOR, G. K. 1952*b* The effect of homogeneous turbulence on material lines and surfaces. *Proc. Roy. Soc.* A **213**, 349.

BATCHELOR, G. K. 1959 Small-scale variations of convected quantities like temperature in turbulent fluid. Part I. General discussion and the case of small conductivity. *J. Fluid Mech.* **5**, 113.

CHATWIN, P. C. & SULLIVAN, P. J. 1979*a* The relative diffusion of a cloud of passive contaminant in incompressible turbulent flow. *J. Fluid Mech.* **91**, 337.

CHATWIN, P. C. & SULLIVAN, P. J. 1979*b* Some diffusion invariants. Submitted to *J. Fluid Mech.*

CORRSIN, S. 1951 On the spectrum of isotropic temperature fluctuations in an isotropic turbulence. *J. Appl. Phys.* **22**, 469.

CRUM, G. F. & HANRATTY, T. J. 1965 Dissipation of a sheet of heated air in a turbulent flow. *App. Sci. Res.* A **15**, 177.

CSANADY, G. T. 1963 Turbulent diffusion in Lake Huron. *J. Fluid Mech.* **17**, 360.

CSANADY, G. T. 1973 *Turbulent Diffusion in the Environment.* Dordrecht: D. Reidel Publishing Company.

MONIN, A. S. & YAGLOM, A. M. 1975 *Statistical Fluid Mechanics: Mechanics of Turbulence, Volume* 2 (ed. by J. L. Lumley). The M.I.T. Press.

MURTHY, C. R. & CSANADY, G. T. 1971 Experimental studies of relative diffusion in Lake Huron. *J. Phys. Ocean.* **1**, 17.

OBUKHOFF, A. M. 1949 Structure of the temperature field in a turbulent flow. *Izv. Akad. Nauk S.S.S.R. Geogr. i Geofiz.* **13**, 58.

SULLIVAN, P. J. 1965 A description of the relative turbulent diffusion of a cloud of marked fluid elements using a distance neighbour function. M.A.Sc. Thesis, University of Waterloo.

SULLIVAN, P. J. 1971 Some data on the distance–neighbour function for relative diffusion. *J. Fluid Mech.* **47**, 601.

SULLIVAN, P. J. 1975 The $\frac{4}{3}$rds. law of relative diffusion. *Mém. Soc. Roy. Sci. Liège*, 6e. *série* **7**, 253.

UBEROI, M. S. & CORRSIN, S. 1953 Diffusion of heat from a line source in isotropic turbulence. *N.A.C.A. Rep.* 1142.